Quantitative characterization of vapour adsorption on solid surfaces and estimation of emissivity of solids using infrared thermography

by B. Vainer

Rzhanov Institute of Semiconductor Physics, Russian Academy of Sciences, Siberian Branch, Novosibirsk, Russia

Abstract

The process of adsorption of water-vapour molecules on uneven (irregular) surfaces of some solid materials at room temperature is registered by infrared camera. The pronounced "thermal flame" ("thermal fire") phenomenon developing on the samples' surfaces is exhibited and quantitatively represented. This thermal effect ranged within an order of magnitude. 3-μm-wavelength emissivities of different fabrics are obtained experimentally with the presented non-standard reflection-based method that needs for a narrow-spectral-range infrared camera. An analytical relationship between the amount of adsorbate and the measurable excess of adsorbent temperature is derived. Exclusively high sensitivity of the FPA-based infrared method as applied to the examination of initial stages of adsorption of gaseous molecules on solid surfaces is discovered. It is shown that the method makes it possible to control an incipient molecular film of 1/300-monolayer effective thickness precipitated on the exposed surface of a bulky material and of 1/600-monolayer thickness in the case of the adsorption on a thin-film adsorbent (with a double-faced surface).

1.   Introduction

Thermal processes in solids, liquids, living tissues, etc. are being studied today with infrared thermography (IRT) [1–4]. IRT provides a means for combining real-time visualization with quantitative analysis. Temperature sensitivity of hundredths of a degree that has become available in the focal plane arrays (FPAs) at frame rates of tens and hundreds of frames per second [5–7] makes FPA-based IR systems very attractive as high-performance experimental means in thermophysical measurements.

At the same time, the well-known problem peculiar to IRT is ambiguity about the sample emissivity (and its associated reflectivity and the ability to absorb the incident flux). It is one of the reasons hampering broad application of IRT to a number of spheres in which a pinpoint accuracy in temperature measurements is required. Notwithstanding the fact that thermograms are normally graded in degrees, an IR camera is normally not considered as a distant thermometer mainly owing to the fact that its sizeable visual field allows objects of different emissivities to fall within its view. Nevertheless, when *a fortiori* known objects are under investigation, their emissivities can be predetermined and the temperatures approaching the absolute ones can be measured. To date, a set of experimental methods aimed at the determination of the emissivity of different materials has been proposed [8]. At the same time, the new ones are as yet in great demand here.

One of the best conditions for application of the infrared camera is when the heat is generated in the immediate region of a surface of a body. In the present work the last situation was maintained. It is sampled in studies of water vapour adsorption on uneven (irregular) surfaces of solid materials. Deposition of molecules onto any type of surfaces from a gas (vapour) phase (adsorption, condensation) is of considerable current interest in many scientific and technical applications. It plays a crucial role in heat exchange processes, biochemical systems, etc. Of special interest is the study of adsorption mechanisms of water [9,10].

The present work comprises both the review of our the latest results [11] and the all-new material on the above-mentioned subjects.

2.   "Thermal flame" ("Thermal fire") phenomenon

Adsorption manifests itself where surface phenomena are to be important. In this section, on the basis of new experimental data, we present evidence that IRT is useful as a convenient scientific instrument both in the investigation of adsorption (condensation) itself and in the characterization of physicochemical and structural features of surfaces where adsorption occurs.

With the help of the FPA-based IR camera described in [6], we studied the release of phase transition heat in the non-equilibrium process of deposition of fast molecules escaped from the liquid (water) to the nearby surface of solid bodies of variable chemical compositions and topological structures. A set of different types of samples of fabric was selected for the adsorbents. We first demonstrated this effect in [12] when used the evaporation-test cell.

In the course of the experiment we immersed the weighted lower edge of a fabric ribbon into an experimental dish filled with water of room temperature or lower (16–18°C). Immediately afterwards, the evolution of the thermal pattern springing up on the ribbon surface above the water-fabric interface was detected every 1 second by the IR camera. Several types of swatches made from various fibres were subjected to this test. There

were swatches both of natural fabrics (lawn, cotton, flannel, velveteen, poplin, linen crinoline, silk cloth, woollen cloth) and of artificial and composite ones (polyamide, polyester, jean cloth, factory cloth tape, etc.).

A distinguishing feature of the effect observed in the experiment was the pronounced rise in temperature of a fabric surface in a quite limited zone above the front of the liquid soaking into the swatch. This phenomenon is demonstrated in figure 1. Quantitative characteristics of the observed thermal pattern are drastic increase in temperature from below (liquid side) and, then a smooth fall in the temperature upwards. A similar effect (heat front propagation) was also distinctly observed in the radial direction by a local moistening of linen or absorbent paper stretched flat (figure 2). In figure 3, some examples of the "thermal flame"-phenomenon manifestations observed on the surfaces of different specimens are shown. The diagram given in figure 4 and related to a polyester fabric at three points in time gives an accurate account of the effect.

To gain a better insight into the mechanism of the "thermal flame" ("thermal fire") observed in figures 1–3, a series of experimental tests was performed using water of different temperatures as well as ethyl alcohol or olive oil as alternative liquids. A conceivable heating of fabric due to its mechanical deformation [13] was also put to the test and eliminated from consideration as negligible for our experiments. As a result, we came to recognize that this phenomenon is most likely to be conditioned by heat generation accompanying the adsorption of water vapour by the solid material surface (the adsorption heat release). The heat effect fading out with time (see figures 1 and 4) probably results from the establishment of an adsorption-desorption balance on the surface.

Figure 4 can serve as a confirmation that it is the rise in temperature that is responsible for the origin of "thermal flame", not, for instance, the change in fabric surface emissivity due to the precipitated film of water. Indeed, it is obvious that the piece of a fabric corresponding to the part of graphic marked by a horizontal bracket is more moistened at time t = 153 s than at t = 21 s. In spite of this fact, we can see that the "fire"-effect is fading down with time to the initial state of the fabric surface. Some additional confirmations are presented in [11].

We observed a very interesting effect when covered two experimental dishes by a flannel fabric. Preliminarily, one of the dishes was filled with cold water (below room temperature), another with spirit at room temperature. In figure 5 the temperature increase registered on the fabric side opposite to the surface facing the water is observed. It can be interpreted as a "thermal fire" effect (adsorption of water molecules on the fabric surface from the inside of the dish). On the contrary, the fabric temperature in the part located above the spirit is decreased. It is well known that the spirit has less adsorption heat as compared with water. The atmosphere under the fabric above the spirit contains many molecules of spirit and few molecules of water. It results in the desorption of equilibrium-conditioned water molecules (absorbed previously owing to the surrounding air moisture) from the inner (predominantly) surface of the fabric. The heat balance leads to the fabric temperature decrease.

It should be noted that the temperature values shown in figure 4 are conventional. They represent the readings of the IRT system calibrated beforehand by a blackbody rather than the actual fabric temperature. To calculate the real temperature, it is necessary to consider the emissivity of the textile surface. A more thorough quantitative analysis calls for taking into account possible peculiarities of angular radiation distribution, as well as possible emissivity variation in the process of the experiment caused by water molecules' precipitation on the surface and the increase in the sample temperature. At low vapour pressures of the liquid (cold water) and insignificant variations in temperature, as in figure 4, it is doubtful that the above effects can make a significant contribution to the main result given in figures 1–3.

Below we describe the experimental procedure aimed at obtaining the emissivity estimate of the fabrics studied.

3. Estimation of emissivity of solids and evaluation of the object real temperature using a narrow-band infrared camera

As suggested in [14], a quadratic trinomial $U_i = \alpha_i T_i^2 + \beta_i T_i + \gamma_i$ is a close approximation of a signal (U_i) – temperature (T_i) dependence measured for each photosensitive cell with number i in the course of the black-body-based laboratory calibration of the FPA-camera used in this work. Here, α_i, β_i, and γ_i are the constant coefficients experimentally obtained for the i-th cell. Temperature T_i associated with a pixel i is easily evaluated by a camera computing system at any time by resolving the quadratic equation written above.

In the course of IR camera ordinary work, the total signal $U_i = U$ measured by arbitrary photosensitive cell with coefficients $\alpha_i = \alpha$, $\beta_i = \beta$, and $\gamma_i = \gamma$ is composed of two components. One (U_R) is determined by thermal radiation of the sample at temperature T. Another (U_B) is determined by background radiation received by the sample from the surrounding bodies at temperature T_B and reflected from its surface. To exclude from consideration the contribution of radiation passed through the sample under study, we shall treat it as rather thick and thus opaque.

It is important that photodetectors used in this work have a narrow spectral sensitivity band $\Delta\lambda$, so the following condition is satisfied [14]

$$\Delta\lambda << \lambda_0 \qquad\qquad (1)$$

where λ_0 is the characteristic operating wave length of the IR camera (in our case about 2.8 μm). Taking into account that the photodetectors used (InAs based metal-insulator-semiconductor structures operating as charge-injection devices) are of photonometric type, fact (1) allows one (in estimate calculations) to consider the signal U to be proportional both to the number of photons and to radiation energy. So we can write:

$$U_R = \varepsilon U_{RBB} = \varepsilon(\alpha T^2 + \beta T + \gamma) \qquad ,$$

$$U_B = (1-\varepsilon)\varepsilon_B U_{BBB} = (1-\varepsilon)\varepsilon_B(\alpha T_B^2 + \beta T_B + \gamma) \qquad ,$$

where ε is the emissivity of the sample under investigation which may be treated as the spectral radiation coefficient by virtue of (1), ε_B is the emissivity of background objects (for instance, the walls of the room where measurements are made) and U_{RBB} and U_{BBB} are photoresponses that could be detected by the IR camera during its calibration, if the calibrated source (blackbody) was heated to T or T_B, respectively. Thus

$$U = \alpha T_M^2 + \beta T_M + \gamma = \varepsilon(\alpha T^2 + \beta T + \gamma) + (1-\varepsilon)\varepsilon_B(\alpha T_B^2 + \beta T_B + \gamma) \qquad (2)$$

where T_M is the temperature displayed by the IR system instead of real temperature T. The main flow of background radiation in IRT measurements under laboratory conditions is brought about by coloured walls of the building. Emissivity of a great number of finishing paints, as well as paper (wall paper) is close to 1. We put $\varepsilon_B \cong 1$ to make further estimations.

Note that if a sample is confined in an isolated place protected from powerful sources of external radiation for a long time, it attains thermodynamic equilibrium with the environment, and its actual temperature T becomes equal to T_B. Simultaneously, according to (2), the condition $T_M = T$ starts to hold, i.e. the IR system begins to show the real temperature of the sample, whatever the emissivity of its surface. Under given conditions, the temperature contrast between the sample and the background almost disappears; this is verified experimentally. The influence of the sample emissivity becomes noticeable when the sample temperature deviates from the equilibrium temperature.

Expression (2) may be recast as

$$T - T_B = \frac{T_M - T_B}{\varepsilon} \cdot \frac{\alpha(T_M + T_B) + \beta}{\alpha(T + T_B) + \beta} \qquad . \qquad (3)$$

Since the difference between the values of T and T_M is almost always substantially less than the sum $(T_M + T_B)$, the last fraction in (3) may be put equal to 1. This yields a very simple relation between the measured and real excess of the sample temperature over the background one:

$$T - T_B = \frac{T_M - T_B}{\varepsilon} \qquad . \qquad (4)$$

Now we describe a possible way of determining ε. Assume that along with equilibrium background radiation there is an additional source of thermal radiation of temperature T_I directed to the sample. The sample itself is of the temperature of the environment $T = T_B$. Then, in view of (2), the signal measured by IRT system

$$U_I = \alpha T_M^2 + \beta T_M + \gamma = (\alpha T_B^2 + \beta T_B + \gamma) + (1-\varepsilon)\chi_I(\alpha T_I^2 + \beta T_I + \gamma) \qquad , \qquad (5)$$

where χ_I is the coefficient making allowance both for emissivity of additional thermal source surface and the fraction of its radiation received by the sample. Express the parameter ε (from (5)) as

$$\varepsilon = 1 - \frac{\alpha(2T_B + \Delta T) + \beta}{\chi_I(\alpha T_I^2 + \beta T_I + \gamma)}\Delta T \qquad , \qquad (6)$$

where the designation $\Delta T = T_M - T_B$ is introduced. Taking into consideration that under real experimental conditions, maximum values of ΔT are commonly slightly different from 1 °C, and, therefore, much less than $2T_B$, we arrive at the expression

$$\varepsilon = 1 - k(T_M - T_B) \qquad , \qquad (7)$$

where k is a coefficient remaining constant in the course of the experiment in which parameters of illumination from the additional source and room background temperature do not change.

Let the value of ε for some material under study be known from independent measurements or the literature. Denote it by ε_d, and the IRT system indication corresponding to this material by T_{Md}. Then expressing k in (7) via the designations introduced, we eventually have

$$\varepsilon = 1 - \frac{1 - \varepsilon_d}{T_{Md} - T_B}(T_M - T_B) \qquad . \qquad (8)$$

Note that finding ε by reflection is preferable to the methods implying detection of thermal radiation on sample heating. Increasing the radiator temperature, one can increase the accuracy of measurements without damaging the material under study and not changing the values of its emissivity under temperature variation.

Expression (8) was employed to determine the emissivity of the fabric samples studied. The source of additional radiation was heated up to the temperature of about 150 °C and was located at several meters from the

set of samples. A number of tests with different additional illumination conditions have been conducted. For each sample values (T_M – T_B) were measured. As a material specifying the reference point (datum point), polyester was chosen for which [8] gives the value of ε_d equal to 0.7 for the wavelength of 3 μm. The difference is that [8] considered white polyester, while we studied polyester fabric of red colour. Table 1 gives the results of emissivity measurements.

Table 1 also represents several characteristic values of excess ΔT of ribbon temperature at the maximum with respect to the temperature at a ribbon point located far from the fabric-liquid interface. Values of ΔT are refined in view of formula (4) and the experimentally obtained ε values; thus they are close to real temperature values. Fabrics are arranged within the row according to the increase in maximum ΔT. A considerable discrepancy between sequences of material alternation in the rows of Table 1 with monotonical increase in ΔT or ε argues for the fact that the difference in measured ΔT for different materials is caused by different heating rather than by different values of ε of fabrics under similar heating.

The time lag between the sample immersion into the liquid and maximal ΔT indication varied from 3 s (thin silk) to 17 s (thick woollen cloth) exhibiting a tendency to increase with the fabric thickness. There is no escape from the conclusion experimentally verified by the presented IR measurements that at equal initial temperatures of the adsorbing surfaces the rate of adsorption depends dramatically on the surface content and structure. It can be seen from Table 1 that ΔT is subject to wide variations, of an order of magnitude. This fact shows high sensitivity of the described IR test and gives birth to hopes for its large scale use in appropriate domains of applicability.

In particular, the possibility of using the given results directly in the textile and knitting industries is noteworthy. For instance, one of the major operations that have been applied in the above-mentioned industries is quality control of manufactured fabrics. Manufacturers are concerned with material porosity, friability, downiness, hairiness, etc. A lot of methods are devised for fabric testing. Certain efforts have been made to incorporate IR cameras into these tests [13, 15]. With these cameras, heating of manufactured articles and materials under deformation has been investigated, permeability of sailcloths has been studied, the coefficient of heat transmission has been measured, etc. It is expected that the physical principle found in this work that allows establishing a hierarchy of tested fabrics (Table 1) will find its application to practice. Moreover, figure 1 demonstrates that the rate of water imbibition into material pronouncedly exhibited by the black area (water) front propagation upwards and characterizing wettability, capillary and absorptive properties of the material is also easily accessible to IR control.

It should be noted that the adsorption/absorption caused textile temperature increase has been a longstanding problem. In [16], the thermal effect was obtained by winding a platinum wire into the wool and using this as a resistance thermometer.

Table 1. Experimentally obtained parameters of different fabrics.

Fabric	max ΔT, °C	Emissivity (λ = 2.8 μm)
Polyamide	0.59	0.692 $\pm$ 0.012
Factory cloth tape	2.41	0.722 $\pm$ 0.012
Crinoline (linen)	2.66	0.732 $\pm$ 0.002
Velveteen (thin)	2.90	0.756 $\pm$ 0.008
Jean (composite cloth)	3.04	0.813 $\pm$ 0.013
Silk cloth	3.22	0.749 $\pm$ 0.012
Velveteen (thick)	3.55	0.750 $\pm$ 0.015
Polyester	3.86	0.7 (datum point)
Half-woollen cloth	3.98	0.780 $\pm$ 0.006
Thick woollen (100%) cloth	4.38	0.762 $\pm$ 0.013
Poplin (cotton)	7.75	0.710 $\pm$ 0.013
Flannel	8.06	0.668 $\pm$ 0.008

4.   Evaluation of the IRT method threshold sensitivity

Accepted laboratory methods of investigation of adsorption, such as surface conductance measurements [17], make possible the registration of the adsorbed layer thickness starting typically from a monolayer. Let us make an evaluation of the sensitivity accessible to the IRT method equipped with the new generation FPA-based IR camera when applied to registration of thermophysics processes accompanying adsorption. To accomplish this, we consider adsorption of gaseous-phase atoms (molecules) by the plane surface of a heat-insulated solid substrate put, for simplicity's sake, into an atmosphere of rarefied air (vehicle) into which the gaseous adsorbate is admitted. Our interest is in the estimation of how many adsorbate monolayers should be accumulated by the adsorbent surface before registration of this initial stage of adsorption becomes accessible to the IR camera.

Let us consider two adsorption conditions: 1) molecules precipitate on a single open side of a "bulky" material (or more exactly on a surface of a thin-film adsorbent closely attached to a "bulky" material and

separated from its heat-conducting body by a heat-insulating layer) and 2) molecules precipitate on both open surfaces of a thin-film solid adsorbent. Let introduce the factor η which takes the value 1 in the first case and 2 in the second case. Let N molecules of the matter with molecular mass μ be sorbed on the surface of area S (it is the area of one of two possible open surfaces). Respectively, the mass of the sorbed molecules is $m = (N/N_A)\mu$, where N_A is the Avogadro constant. Let r be the specific adsorption heat. Then the sorption of N molecules leads to heat evolution

$$Q_1 = rm = \frac{rN\mu}{N_A} \qquad . \qquad\qquad (9)$$

With neglect of heat transmission into environment (rarefied gas), this heat will be consumed to the substrate (adsorbent) heating. We take the substrate mass as M, specific weight of its material as ρ, specific heat as c and thickness as d. Then the heat-balance equation gives

$$\eta Q_1 = cM\Delta T = cSd\rho\Delta T \qquad\qquad (10)$$

where ΔT is the substrate change in temperature owing to the inflow of adsorption heat.

Let us consider a non-steady process on the assumption that the substrate heated in such a manner reverts to the state of thermodynamic equilibrium with the environment after a lapse of time t during which it dissipates the acquired heat ηQ_1 predominantly in the form of electromagnetic radiation. The duration t is determined by emissive power P irradiated from a unit of area into spatial angle 2π that is governed by the Stefan-Boltzmann low $P(T) = \varepsilon\sigma T^4$, where σ is the Stefan-Boltzmann constant, ε the emissivity of the substrate surface and T the substrate temperature. On the estimate level, let assume ε to be of the same values for open and buried adsorbent surfaces alike.

The heat $Q = \eta Q_1$ thus dissipated may be approximated by the expression

$$Q = [P(T + \frac{1}{2}\Delta T) - P(T)]\, 2S\, t \qquad . \qquad\qquad (11)$$

Factor 1/2 before ΔT takes qualitatively into account the fact that the substrate temperature excess over the equilibrium temperature does not remain constant as the adsorbent cools down but diminishes monotonically from ΔT to 0 and is characterized by the average value of $\Delta T/2$. The subtrahend $P(T)$ in (11) allows for the inflow of thermal radiation to the substrate from the environment that is kept at the equilibrium temperature T.

From (9) and (10) we obtain

$$\Delta T = \frac{\eta rN\mu}{N_A cM} = \frac{\eta rN\mu}{N_A cSd\rho} = \frac{\eta rn\mu}{N_A cd\rho} \qquad . \qquad\qquad (12)$$

Equations (9) and (11), in view of (12), give

$$t = \frac{cM}{4\varepsilon\sigma ST^3} = \frac{cd\rho}{4\varepsilon\sigma T^3} \qquad . \qquad\qquad (13)$$

Here, the requirement $\Delta T \ll T$ is taken into account, and a new parameter $n = N/S$, surface density of sorbed molecules, is introduced. From (12) and (13) we have

$$n = \frac{4N_A\varepsilon\sigma T^3}{\eta r\mu}\, t\, \Delta T \qquad . \qquad\qquad (14)$$

With relationship (14) it becomes possible to make a lower estimate of the minimal quantity of adsorbate that the IR camera is able to register because the parameter t is limited from below by the reciprocal of the camera maximum frame rate, and the minimal ΔT to be measured is dependent on the camera sensitivity (noise equivalent temperature difference). Consider, for definiteness, the adsorption of water vapour on the adsorbent surface of $\varepsilon = 0.8$ emissivity and $T = 300$ K temperature. In this case, we can set in (14) $r = 4.4 \times 10^6$ J/kg and $\mu = 18 \times 10^{-3}$ kg/mole. Substituting the values $t = 10^{-2}$ s and $\Delta T = 10^{-2}$ K typical of standard FPA-based IR cameras in (14) gives $n = 2 \times 10^{15}$ m^{-2} (when $\eta = 2$). It is equivalent to the precipitation of one molecule of water on a fragment of the substrate surface composed of 5×10^4 atoms.

In spite of such an impressive result, the questions remain: how long will it take the substrate to get cold after nS (or $2nS$) molecules of the adsorbate are attached to the substrate? Can it happen that this time will turn out to be much less than the minimal exposure technically available to the IR camera? Another point to be mentioned is that aspiration for lower t in response to the increase in the camera frame rate inevitably results, according to (13), in the requirement of the diminution of M/S (or d), and manufacturing such thin substrates may become unattainable.

To make estimation valid and realistic, let us substitute judiciously chosen parameter values in (13). The following values are assigned to the parameters: $c = 1000$ J/(kg K), $\rho = 400$ kg/m^3, $d = 10^{-5}$ m, $T = 300$ K and $\varepsilon = 0.8$. This results in $t \approx 0.75$ s. In view of the above-mentioned frame time 10^{-2} s typical of the standard FPA-based IR camera, the last results show that the adsorptive-thermal effect and the kinetics of its development can be registered by IR camera with a high degree of accuracy.

Rearranging (14) in view of (13) gives

$$n = \frac{cd\rho N_A}{\eta r \mu} \Delta T \qquad . \qquad (15)$$

Relation (15) sets up a correspondence between experimentally registered temperature deviation (excess) of the adsorbent surface and the degree of occupation of this surface by sorbed molecules (atoms). The inverse ratio $\Delta T(n)$ derived from (15) can be called "thermal index of adsorption". When, in actual practice, an IR camera is knowingly designed for control of adsorption processes, this ratio can mediate a calculation of the corresponding calibration factor for those measurements.

Substitution of the same parameters in (15) as were substituted in (13) and also substitution of $r = 4.4 \times 10^6$ J/kg (water vapour), $\mu = 18 \times 10^{-3}$ kg/mole (water) and $\Delta T = 10^{-2}$ K in (15) give us the realistic values $n = 3 \times 10^{17}$ m^{-2} (for $\eta = 1$) and $n = 1.5 \times 10^{17}$ m^{-2} (for $\eta = 2$). In view of the fact that one square meter of the solid surface contains approximately 10^{20} atoms of matter, the obtained values n distinctly show that the characteristic effective sensitivity of the described IRT method expressed in terms of the ratio between the IR camera registered number of adsorbate molecules and the number of adsorbent surface atoms can reach a value as small as 1/300 monolayer (!) for "bulky" specimen and 1/600 monolayer (!!) for a thin-film adsorbent (with a double-faced surface).

5. Conclusions

IR monitoring is best suited to miscellaneous applications in physics. Disclosure and development of new fields of application of IR cameras to experimental physics not only give a chance to open up a new area to the experimenter but also open the way for replacing outmoded facilities and methods by more handy, sensitive and fast means offering the benefit of greater reliability. Specifically, IRT offers undoubted advantages over thermo-visualizing techniques based on the use of liquid crystals. The results of this work show that the IRT method equipped with new-generation FPA-based IR cameras can serve as an adequate scientific instrument in precise thermophysics experiments, and it is suitable for revelation and recognition of fine natural phenomena accompanied by emission of heat.

Generation of heat on the surface of varied fabrics put partly into water is experimentally registered, visualized and quantitatively represented. The thermal effect is ascribed to adsorption of water molecules on the free (dry) surface of fabrics. In spite of quite a low temperature (less than room temperature) of the vaporizing liquid, pronounced heating of the adsorbent surface ("thermal flame" or "thermal fire") was detected. The thermal effect ranged within an order of magnitude depending on the fabric content and the surface structure (irregularity). Registered by the infrared camera, the higher (lower) temperature in the process in question points to higher (lower) adsorption capacity of the investigated materials at room temperature and low partial pressures of gaseous adsorbate. Emissivities of different fabrics are obtained experimentally with the reflection method based on narrow spectral range IRT.

The thermal effect as severe as in figures 1–4 leads one to think about the appropriateness and correctness of the established term "adsorption isotherm". In consequence of the intense heat of the adsorbate-adsorbent interaction zone (especially in chemisorption processes), such diagrams can hardly be considered isotherms. In this regard, what data have come to hand are highly instructive. They pictorially make it clear that experimental conditions require thorough control while the diagrams are measured. The same is also true for the study of condensation. The IR camera can serve here as an appropriate supervisory instrument.

Since the pronounced thermal effect demonstrated in figures 1–3 is dramatically dependent on the hydrophobic (hydrophilic) behaviour of the interfacial surface, it allows one to perform macro-visualization of the time history of the processes occurring on the surface at the nanoscale. In this work, simple analytic expression is derived that establishes a one-to-one correspondence between the quantity of adsorbed matter and the above-equilibrium excess of the adsorbent temperature measured by the IRT system. The quantitative estimation has shown that with the use of FPA-based infrared cameras it is possible to examine the initial stages of adsorption even from the moment when the effective thickness of the adsorbed molecular film is as small as 1/300 of monolayer. This intriguing result provides strong evidence that FPA-based IRT offers the greatest promise as an experimental tool in physics of surfaces and molecular physics.

REFERENCES

[1] P. Cerisier, S. Rahal, and N. Rivier. Topological correlations in Benard-Marangoni convective structures, *Phys. Rev. E*, 54 (1996) 5086–5094.
[2] T. Eich, A. Herrmann, J. Neuhauser, and ASDEX Upgrade Team. Nonaxisymmetric energy deposition pattern on ASDEX upgrade divertor target plates during type-I edge-localized modes, *Phys. Rev. Lett.,* 91 **(**2003) 195003.
[3] A. Bendada, C. Q. Zheng, and N. Nardini. Investigation of temperature control parameters for inductively heated semi-solid light alloys using infrared imaging and inverse heat conduction, *J. Phys. D: Appl. Phys.,* 37 (2004) 1137–1144.
[4] B. G. Vainer FPA-based infrared thermography as applied to the study of cutaneous perspiration and stimulated vascular response in humans, *Phys. Med. Biol.*, 50 (2005) R63–R94.

[5]   G. Destefanis, P. Audebert, E. Mottin, and P. Rambaud. High performance LWIR 256×256 HgCdTe focal plane array operating at 88 K, *Proc. SPIE,* 3061 (1997) 111–116.

[6]   G. L. Kurishev, A. P. Kovchavtzev, B. G. Vainer, A. A. Guzev, V. M. Bazovkin, A. S. Stroganov, I. M. Subbotin, I. M. Zakharov, V. M. Efimov, K. O. Postnikov, I. I. Lee, N. A. Valisheva, and Z. V. Panova. Medical infrared imaging system based on a 128×128 focal plane array for 2.8–3.05 μm spectral range, *Optoelectronics, Instrumentation and Data Processing (Autometria)*, 4 (1998) 5–10.

[7]   A. Manissadjian, P. Tribolet, P. Chorier, and P. Costa. Sofradir infrared detector products: the past and the future, *Proc. SPIE,* 4130 (2000) 480–495.

[8]   C. Salvaggio, and C. J. Miller. Comparison of field and laboratory collected midwave and longwave infrared emissivity spectra / data reduction techniques, *Proc. SPIE*, 4381 (2001) 10 pp.

[9]   R. Sh. Vartapetyan, and A. M. Voloshchuk. The mechanism of the adsorption of water molecules on carbon adsorbents, *Russ. Chem. Rev.*, 64 (1995) 985–1001.

[10] J.-H. Cho, L. Kleinman, K.-j. Jin, and K. S. Kim. Theoretical study of water adsorption on the Ge(100) surface, *Physical Review B*, 66 (2002) 113306.

[11] B. G. Vainer. Focal plane array based infrared thermography in fine physical experiment, *J. Phys. D: Appl. Phys.*, 41 (2008) 065102 (12 pp).

[12] B. G. Vainer. Investigation of cutaneous perspiration and fatty secretion using the infrared thermography method, In: Quantitative InfraRed Thermography 6, QIRT'02, Dubrovnik, Croatia. September 24–27. Book of Abstracts. University of Zagreb (2002) 123–125.

[13] Z. Mikolajczyk, B. Wiecek, and M. Michalak. Thermovision method in stress analysis of textile materials, In: Proc. of the 60th Eurotherm Seminar on Quantitative InfraRed Thermography, QIRT'98, Lodz, Poland, 1998, Ed. D. Balageas, G. Busse and G. M. Carlomagno (Poland: PKOpto SEP) (1998) 140–146.

[14] B. G. Vainer. Narrow spectral range infrared thermography in the vicinity of 3 μm operating wavelength, In: Quantitative InfraRed Thermography 5, QIRT'2000, Reims, France, July 18–21. Proceedings. UTAP URCA (2000) 84–91.

[15] M. Zimniewska, M. Michalak, I. Krucinska, and B. Wiecek. The physical properties of the surface of apparel made from flax and polyester fibres, *Int. J. Clothing Sci. Technol.*, 15 (2003) 284–294.

[16] A. B. D. Cassie. Physics and textiles, *Rep. Prog. Phys.*, 10 (1944) 141–171.

[17] Y. Awakuni, and J. H. Calderwood. Water vapour adsorption and surface conductivity in solids, *J. Phys. D: Appl. Phys.* 5 (1972) 1038–1045.
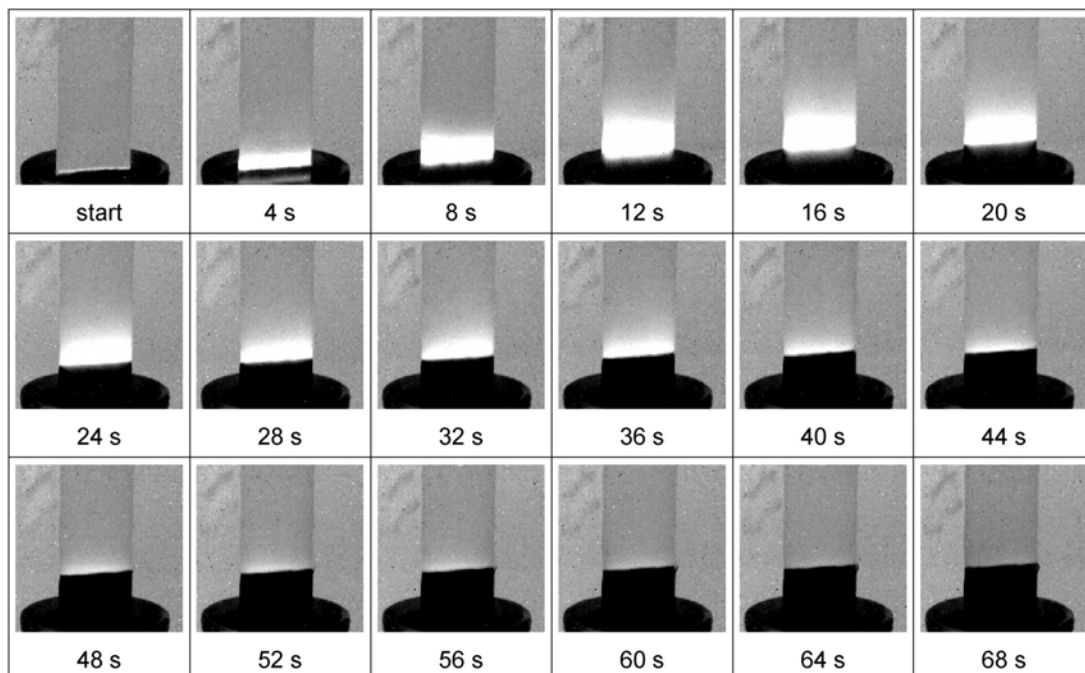
Fig. 1. *Heat generation ("Thermal flame" or "Thermal fire") caused by adsorption of water molecules on the surface of cotton fabric (poplin) after immersion of the fabric edge into liquid water. The time elapsed since the fabric moistening is indicated under each corresponding thermogram.*
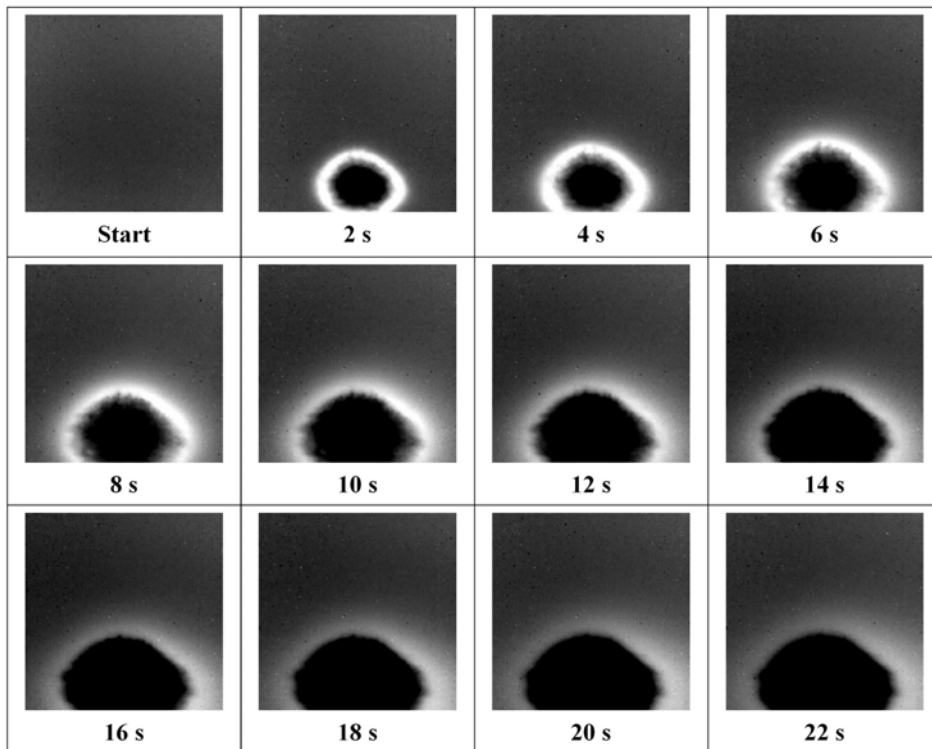
Fig. 2. *"Thermal flame" ("Thermal fire") phenomenon on the flannel surface stretched aflat. The time elapsed since a fabric moistening is indicated under each corresponding thermogram.*
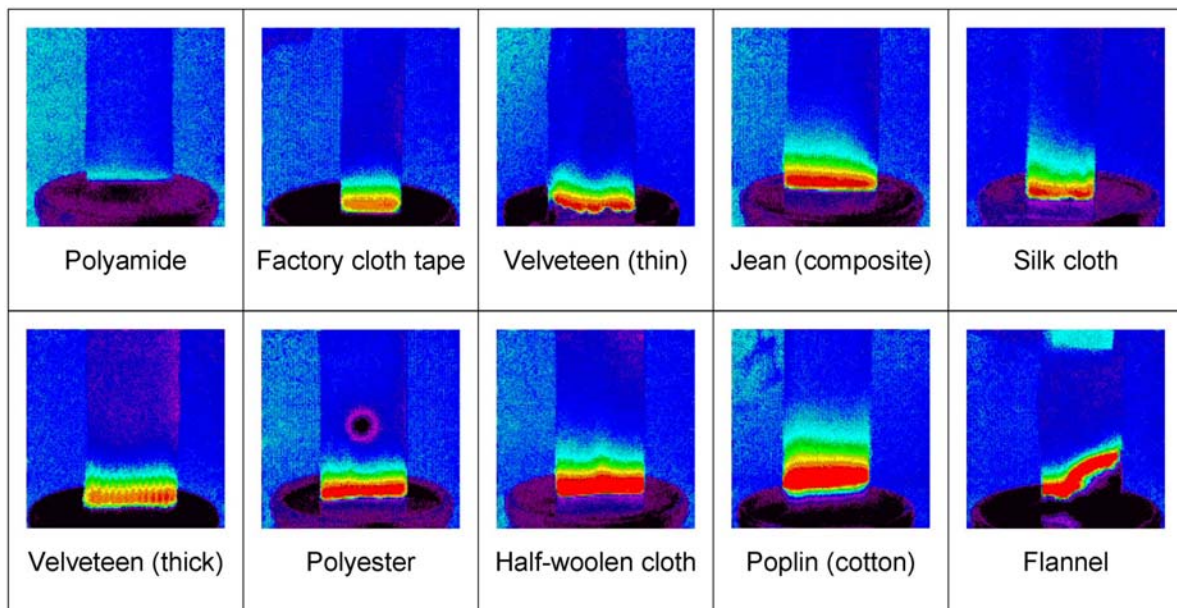
Fig. 3. *"Thermal flame" / "Thermal fire" phenomenon observed on the surfaces of different fabrics.*
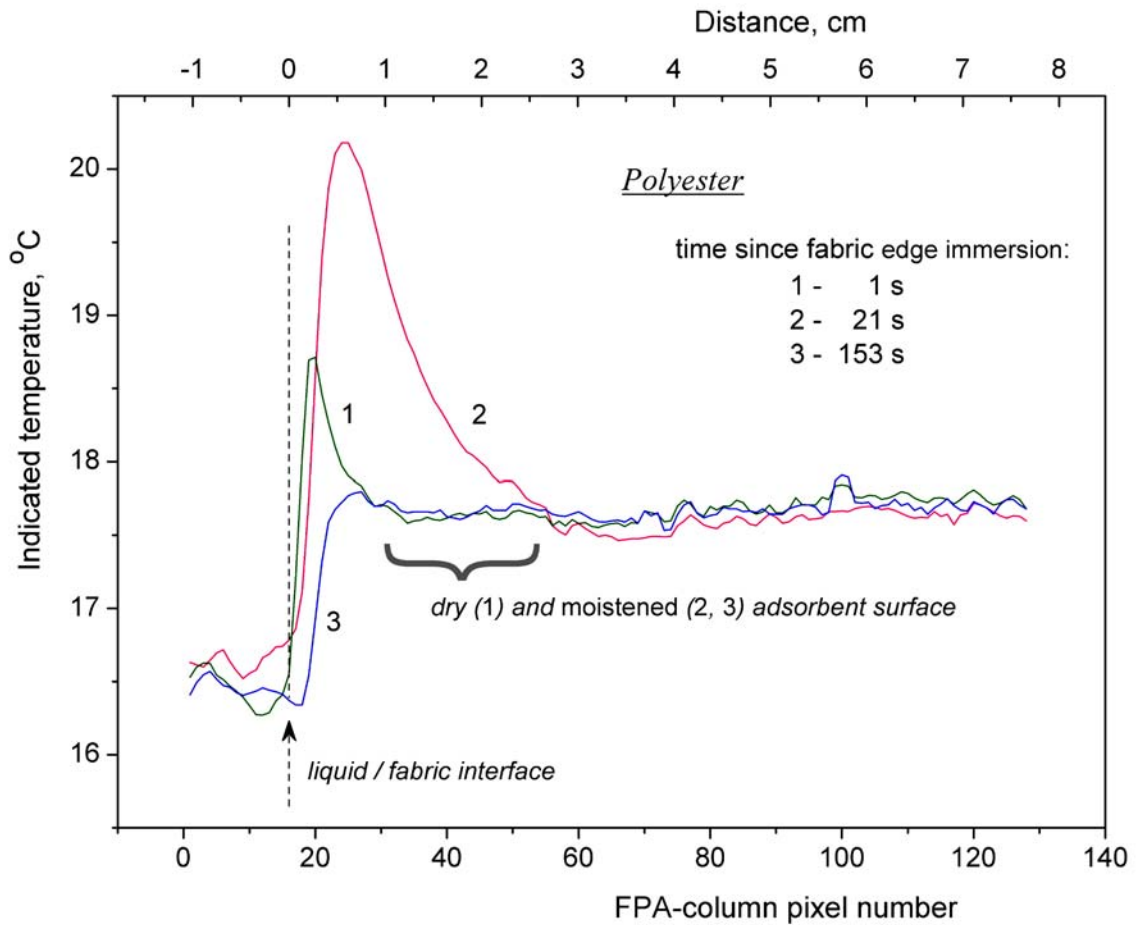
Fig. 4. A quantitative characteristic of the effect exhibited in figures 1 and 3; it demonstrates
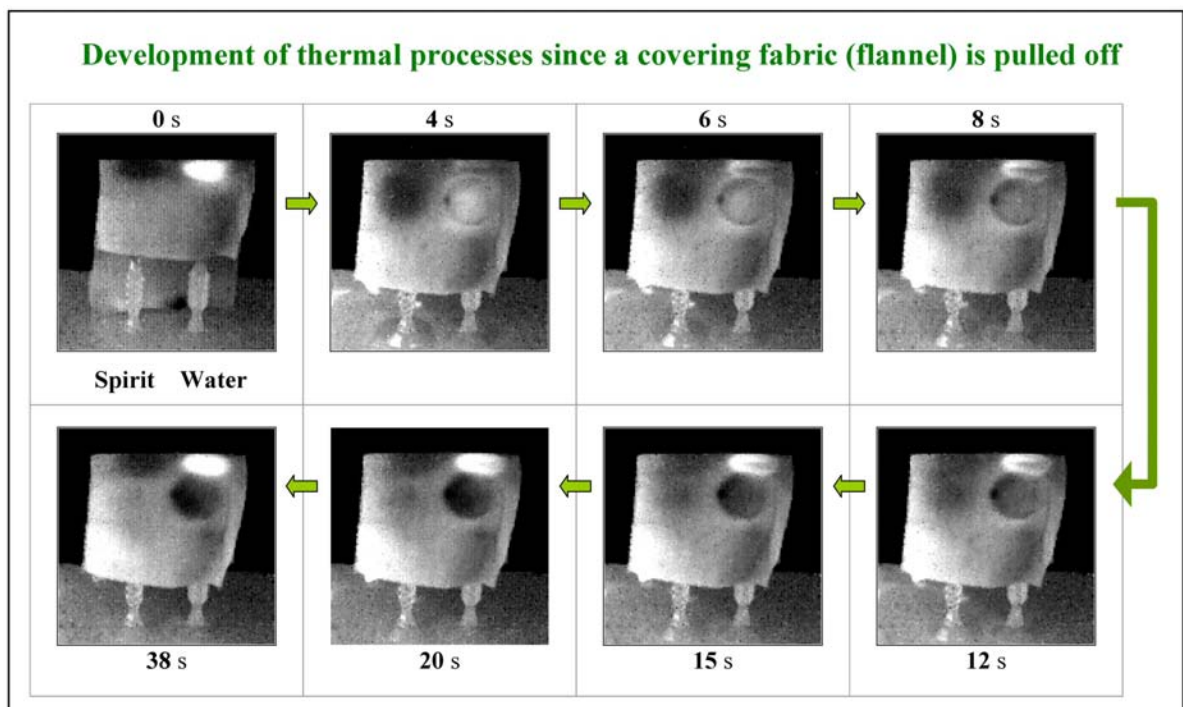a typical temperature distribution along the down-top section of the thermograms.

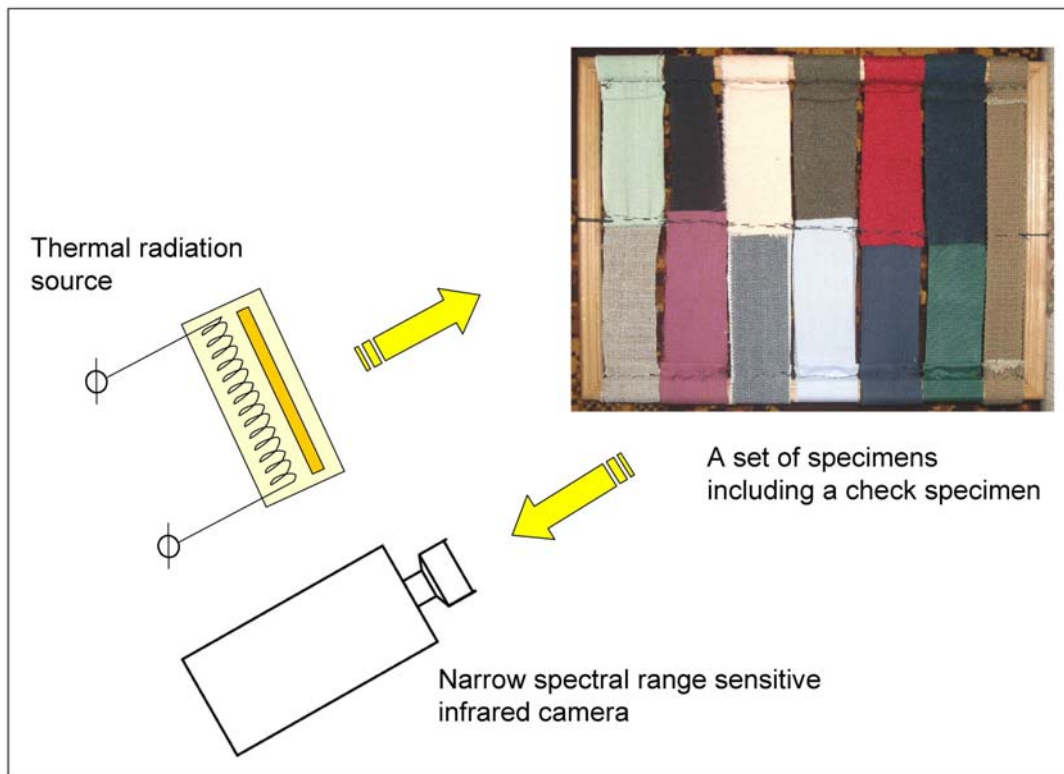**Fig. 5.** *Two adsorption/desorption-conditioned thermal effects which are the reverse of each other.*

Fig. 6. A conceptual sketch of the test setup meant for the measurement of emissivity.
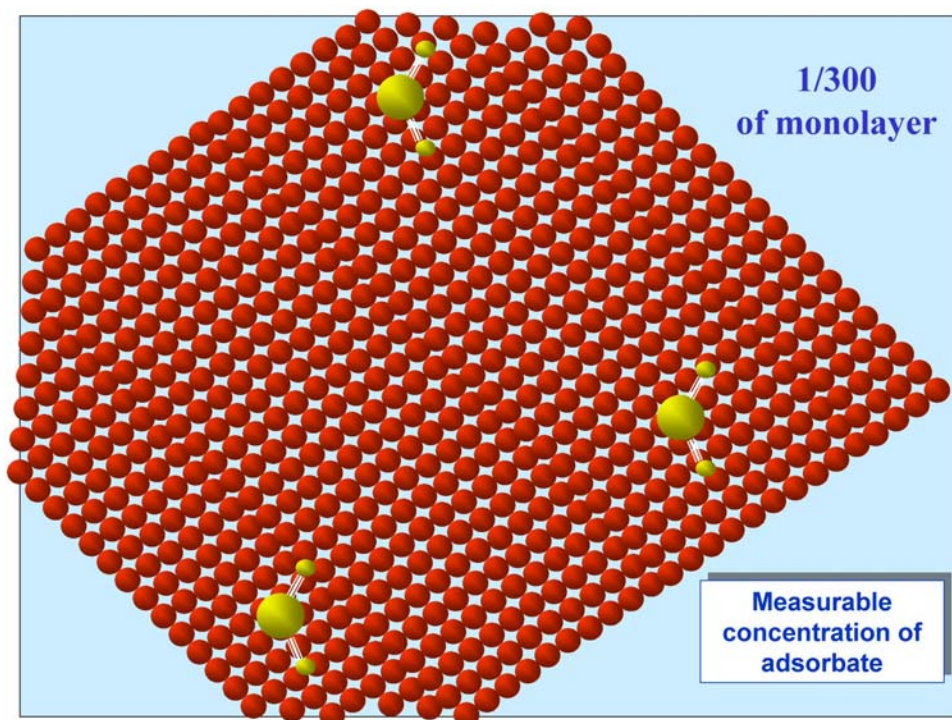

Fig. 7. Pictorial presentation of the FPA-based infrared thermography sensitivity.
Red – surface atoms of a solid, yellow – adsorbed molecules of water.